Fungal Ecology 45 (2020) 100922

Contents lists available at ScienceDirect

Fungal Ecology

journal homepage: www.elsevier.com/locate/funeco

Rapid changes in the chemical composition of degrading ectomycorrhizal fungal necromass

Maeve E. Ryan [a], Kathryn M. Schreiner [a, b, *], Jenna T. Swenson [a], Joseph Gagne [c, d], Peter G. Kennedy [c, d]

[a] Department of Chemistry and Biochemistry, University of Minnesota Duluth, 1038 University Dr., Duluth, MN, USA
[b] Large Lakes Observatory, 2205, E. 5th St., Duluth, MN, USA
[c] Department of Plant and Microbial Biology, University of Minnesota, St. Paul, MN, USA
[d] Department of Ecology, Evolution, and Behavior, University of Minnesota, St. Paul, MN, USA

ARTICLE INFO

Article history:
Received 22 July 2019
Received in revised form
11 December 2019
Accepted 30 January 2020
Available online xxx

Corresponding Editor: Marie Davey

Keywords:
Mycorrhizal fungi
Decomposition
Melanin
Soil organic matter
Necromass chemistry

ABSTRACT

Characterizing the chemical changes in fungal necromass as it degrades, particularly over short time intervals (days to weeks), is critical to clearly understanding how this organic matter source contributes to various belowground carbon and nutrient pools. Using a range of chemical analyses, we assessed the degradation of four types of ectomycorrhizal fungal necromass from three species differing in biochemical composition. Samples were buried in a forest in Minnesota, USA and harvested at eight time points over a 90-day incubation period (1, 2, 4, 7, 14, 28, 60, 90 days). Three of the necromass types lost greater than 50% of their initial mass in the first seven days, but mass loss plateaued for all four types at later harvests, and after 90 days, none of the samples were completely degraded. Relative to undegraded necromass, degraded necromass consistently contained a lower relative abundance of aliphatic compounds and a higher relative abundance of carbohydrates, sterols, and aromatic compounds. For three of the four necromass types, nitrogen content was lower after 90 days of degradation and FTIR spectra revealed distinct peaks broadening from day 0 to day 90. While melanin content significantly slowed degradation within species, differences in degradation rates across species were more closely aligned with initial nitrogen content. Collectively, our results indicate that the rapid mass loss of dead fungal mycelium is accompanied by a wide range of changes in necromass chemistry, likely contributing to both short-term soil nutrient and longer-term carbon pools.

1. Introduction

Twice as much carbon (C) is stored in soil organic matter (SOM) as exists as carbon dioxide in the atmosphere, totaling an estimated 1500 Pg in the top meter of soil globally (Jobbagy and Jackson, 2000). Historically, aboveground plant inputs were considered primary determinants of SOM accumulation in forest ecosystems (Swift et al., 1979), but more recent work has demonstrated that mycorrhizal fungi, via colonized roots and mycelium, represent a considerably larger portion of forest SOM pools than previously recognized (Högberg and Högberg, 2002). For example, it has been estimated that up to 70% of the C in boreal forest soils originates from belowground roots and root-associated mycorrhizal fungal sources (Clemmensen et al., 2013), and, in temperate forests, mycorrhizal fungi have been shown to contribute more to the SOM C pool than leaf litter and fine root turnover combined (Godbold et al., 2006). It has also been demonstrated that degradation-resistant SOM looks more like microbial products than plant products on a molecular level (Simpson et al., 2007; Kallenbach et al., 2016), suggesting the decomposition of microbial tissues (hereafter referred to as necromass) plays an important role in soil C cycling. Collectively, the high proportion of SOM originating from mycorrhizal fungi (either as part of colonized root tips or as extraradical hyphae) along with the demonstrated retention of microbial-derived OM in soils suggest that these organisms represent a prominent component of belowground C storage.

Relative to other SOM inputs, the initial decomposition of fungal mycelium is typically rapid, with significant mass loss (>50%) occurring within the first month of incubation (Fernandez and Koide, 2012; Brabcová et al., 2016, 2018; Certano et al., 2018).

* Corresponding author. 2205 5th St. E, Duluth, MN, 55812, USA.
E-mail address: kschrein@d.umn.edu (K.M. Schreiner).

https://doi.org/10.1016/j.funeco.2020.100922
1754-5048/

The early decay of fungal necromass has been positively correlated with tissue nitrogen (N) concentration (Koide and Malcolm, 2009; Fernandez et al., 2019), but detailed analyses of the chemical changes in necromass, particularly during the first days of decomposition, are currently lacking. It seems likely that much of the N being accessed by microbial decomposers comes from different components of fungal cell walls; either chitin, a biopolymer composed of N-acetylglucosamine monomers, or wall-bound proteins, the latter of which account for up to 70% of fungal cell wall nitrogen (Smiderle et al., 2012). Fernandez and Koide (2012) demonstrated that increased chitin concentration was significantly positively associated with faster rates of fungal necromass decomposition, suggesting chitin is an important N-related resource. However, chitin also contains significant amounts of C and can bind to other C-rich cell wall components, such as glucans, which together represent approximately 80% of cell wall mass (Bartnicki-Garcia, 1968). Using stable isotope probing, Drigo et al. (2012) found that chitin-glucan complexes degrade quickly (within one month), suggesting that labile C sources in fungal cell walls, including chitin, are also targeted during initial fungal necromass decomposition.

The cell walls of many fungi additionally contain melanin, a group of pigments found across biological kingdoms (Henson et al., 1999). Estimates of the amount of melanization vary widely, but in forest soils, it appears that over half of fungal mycelium is melanized (Fogel and Hunt, 1983; van der Wal et al., 2009). Melanin is a biopolymer with a complex, irregular structure of phenolic and indolic monomers, making it highly aromatic (Bull, 1970). The specific chemical structure of fungal melanin is largely unknown, but has been shown to differ among species, and is often complexed with other cell wall components (Butler and Day, 1998). In addition to providing protection from ultraviolet light, drought, and oxidizing agents in the soil (Butler and Day, 1998; Feofilova, 2010; Fernandez and Koide, 2013), melanin has been shown to decrease the rate of degradation of ECM fungal necromass, both within and across species (Fernandez and Koide, 2014; Fernandez and Kennedy, 2018). The mechanism for this inhibition may be due to the inherent recalcitrance of melanin itself (Butler and Day, 1998) and/or inhibitory effects on the extracellular enzymes responsible for breaking down cell wall components, causing chitin, glucan, and proteins to degrade more slowly in its presence (Kuo and Alexander, 1967). Chitinase activity, in particular, can be halted entirely in the presence of melanin (Bull, 1970). Melanin also represents the dominant remaining polymer in necromass following long-term incubation (Fernandez et al., 2019), suggesting its abundance is a key predictor of the C contribution into stable SOM pools.

Given the rapid nature of fungal necromass turnover (Allen and Kitajima, 2013; Hagenbo et al., 2017), characterizing changes in tissue chemistry over short time intervals (days to weeks) is critical to more clearly understanding how fungal necromass C and N contribute to various belowground nutrient and SOM pools. To date, most of the chemical characterization has either been after at least 30 days (Certano et al., 2018; Fernandez et al., 2019) or conducted in laboratory settings (Drigo et al., 2012; Schweigert et al., 2015; López-Mondéjar et al., 2018), where decomposer community composition may differ from natural settings due to the absence of obligate symbioses (Fernandez and Kennedy, 2018; Maillard et al., in review). To address this gap in knowledge, the aim of this study was to profile changes in the chemical composition of ECM fungal necromass throughout a 90-day degradation period, with an enhanced focus on early time points. Specifically, necromass of three species differing in initial melanin and nitrogen contents was sampled at nine points over the 90 day experiment, with increased sampling frequency during the first week of degradation. Chemical changes are analyzed semi-quantitatively by employing both thermochemolysis-gas chromatography-mass spectrometry and Fourier-transform infrared spectroscopy.

2. Methods

2.1. Necromass generation

Necromass of four types (three ECM fungal species) was generated: *Cenococcum geophilum* (CG), *Suillus punctipes* (SP), a high-melanin representative of *Meliniomyces bicolor* – black (MBb), and a low-melanin representative of *Meliniomyces bicolor* - white (MBw). The different representatives of *M. bicolor* were the same strain; melanin content was naturally manipulated based on the degree of submersion of fungal tissue within the growth media, as in Fernandez and Kennedy (2018). Isolates of each species were grown in 50 mL half-strength potato dextrose broth (100 mL for MBw) in 125 mL flasks. Flasks were shaken at 80 RPM at room temperature on orbital shakers for 30 days. Fungal colonies were harvested, rinsed with deionized water, and oven-dried for 24 h at 27 °C. The resulting necromass (21 mg–120 mg) was placed in nylon mesh litter bags (3 × 3 cm, 53 μm mesh), heat-sealed, and each bag was attached to a metal numbered tag for later identification.

2.2. Field degradation

Bags were buried in a *Pinus*-dominated forest at Cedar Creek Ecosystem Science Reserve (45°25′16″ N, 93°11′49″ W) in East Bethel, Minnesota, USA, on June 27th, 2018. The soil in this forest is sandy and contains 0.37% ± 0.14% N and 4.07 ± 1.72% organic carbon. Bags were buried under the litter layer at the litter-soil interface, 10 cm apart in each of four plots, and allowed to degrade naturally thereafter. Each plot was 10 m apart to account for soil and environment heterogeneity. Four replicates of each species on each harvest day (1 per plot) were harvested after 0, 1, 2, 4, 7, 14, 28, 60, and 90 days degradation. Day 0 bags were harvested after spending approximately 1 h in the soil and are considered “control” undegraded samples in this study.

2.3. Sample processing

At harvest, bags were removed from the soil, placed in individual pre-combusted, carbon-free glass jars, and transported on ice back to the lab (a trip of approximately 3 h). Immediately upon arrival at the laboratory, necromass was removed from mesh bags, placed in pre-weighed, pre-combusted 20 mL glass scintillation vials, and frozen overnight. Necromass was then freeze-dried, weighed, and ground to fine powder with a Wig-L-Bug grinding mill. For harvest days 0 through 14, mass loss was determined from pre- and post-incubation dry weights. Samples were stored in glass scintillation vials in a desiccator.

At some point between harvest days 14 and 28, some of the litterbags were removed from the soil, presumably by an animal. By day 60, most of the bags had been moved within the site and were no longer connected to their ID tags. Because of this, it is impossible to know with certainty the initial masses of each collected bag to accurately calculate mass loss. Therefore, mass loss for harvest days 28, 60, and 90 was calculated by averaging the initial masses of the bags remaining of each species and averaging the final masses of bags collected. These data are presented with open circles in mass loss figures.

2.4. Elemental analysis

Elemental analysis (EA) was run on a Costech elemental analyzer (Costech Analytical Technologies, Valencia, CA, USA).

Samples were weighed in tin capsules. A set of standards was run every 10 samples. Standards used were acetanilide (71.09% C, 10.36% N), caffeine (49.48% C, 28.85% N), natural-abundance sorghum (41.58% C), and low-organic content soil (1.61% C, 0.13% N). Standard error was less than 0.6% for %C and 0.4% for %N.

2.5. Thermochemolysis-gas chromatography-mass spectrometry

All necromass samples for which there was sufficient remaining biomass were analyzed by thermochemolysis-GCMS (pyGCMS) (Çoban-Yildiz et al., 2000). Tetramethylammonium hydroxide (TMAH) was added to weighed, ground necromass as a methylating agent. Samples were heated to 300 °C at a rate of 720 °C/min in a Gerstel Thermal Desorption Unit and immediately introduced into the GC column (HP-5MS, 30 m × 0.250 mm, 0.25 μm film thickness). The GC-oven (Agilent Technologies, 7890B, Santa Clara, CA, USA) was heated from 50 °C to 320 °C over 55 min and held at 320 °C for 10 min. Molecules were ionized in an Agilent Technologies 5977A mass spectrometer by electron ionization with a voltage of 70 eV.

Peaks were classified as aliphatics, aromatics, carbohydrates, nitrogen-containing, sterols, or compounds of unspecified origin by their mass spectra using Agilent ChemStation software, standard runs, and the NIST library. Standards included chitin, glucan, mannan, ergosterol, and lignin. Fatty acids and fatty alcohols were included in the aliphatic category. N-containing fragments included proteins and amino sugars; N-containing chitin fragments were included in the N-containing category, not the carbohydrates category. Single ion monitoring (SIM) was performed by Agilent MassHunter software. Relative abundance of each classification of compound was calculated using a MATLAB script (see Supplemental Information).

2.6. Fourier-transform infrared spectroscopy

Ground necromass from all samples was also analyzed with attenuated total reflectance-Fourier transform infrared spectroscopy (ATR-FTIR) (Thermo Scientific, Nicolet iS10, Waltham, MA, USA). Wavenumbers ranged from 40 to 4000 cm^{-1} with a resolution of 4.0 cm^{-1} for 100 scans. Peak areas were deconvoluted and normalized to total peak area using PeakFit software.

2.7. Melanin isolation

Melanin was isolated from ground necromass based on the method of Prados-Rosales et al. (2015). Briefly, approximately 0.5 g freeze-dried necromass was suspended in a solution of phosphate-buffered saline (PBS), buffer (1 M sodium citrate, 0.1 M sorbitol, pH 5.5), and lysing enzyme (10 mg/mL) and incubated at 30 °C for 24 h. The sample was centrifuged to collect the pellet and washed five times with PBS. A 4 M solution of guanidine thiocyanate was added and the sample was incubated at room temperature overnight with constant shaking. After centrifugation and PBS wash, buffer (10 mM TrisHCl, 5 mM calcium chloride, 5% SDS, pH 8.0) and proteinase K (1 mg/mL) were added and it was incubated at 65 °C for 4 h. The sample was centrifuged and the pellet was resuspended in PBS. A solution of methanol and chloroform (2:1 by volume) was added to achieve a final ratio of 4:2:1 chloroform:methanol:water. The chloroform layer was extracted and disposed. The remaining mixture was acid hydrolyzed with 6 M hydrochloric acid and heated for 1 h. The hydrolyzed product was dialyzed (MWCO 12 kDa) against carbon-free MilliQ water for 72 h at 4 °C with constant stirring and daily water changes. The remaining mixture was freeze-dried to collect the melanin. Melanin content is presented as milligrams of melanin per grams of bulk necromass.

2.8. Kinetic modeling and statistical analysis

Degradation rate constants were determined for exponential, Single-G, and Multi-G (biexponential) models. Exponential rate constants k_{exp} were calculated by dividing the natural log of the relative mass remaining after 90 days of degradation by 90 days (Fernandez and Koide, 2014). For the Single-G model, the natural log of the relative mass remaining at each harvest day was plotted versus time (Berner, 1964). The rate constant was the negative slope, determined by linear regression with the y-intercept set to 0. Degradation of each species was fitted with a Multi-G model with two pools of carbon: one fast-degrading and one slow-degrading (Westrich and Berner, 1984). The model was fitted by alternating adjusting the rate constants, k_1 and k_2, and relative amounts of each pool, β_1 and β_2, to minimize the sum of the squared residuals (SSR). The fit was adjusted a total of eight times, at which point the decrease in SSR between iterations was less than 0.001. Statistical significance was determined using single-factor ANOVA with an alpha of 0.05.

3. Results

3.1. Initial melanin and nitrogen content

Melanin content ranged from 7 to 160 mg melanin g^{-1} bulk necromass (Fig. 1a). MBb (*M. biocolor* – black) contained the most melanin at 160 mg melanin g^{-1} bulk necromass, followed by CG (*C. geophilum*) at 93 mg melanin g^{-1} bulk necromass. SP (*S. punctipes*), despite being visually darker than MBw (*M. bicolor* – white), contained the least amount of melanin at 7 mg melanin g^{-1} bulk necromass. Nitrogen content ranged from 2.81% to 4.99%, with MBb containing significantly less nitrogen than the other necromass types ($p < 0.05$; Fig. 1b). The C:N ratio of undegraded necromass ranged from 8.5 to 18.6, with MBb having a significantly higher C:N ratio than the other three types at 18.6 ± 3.8 ($p < 0.05$).

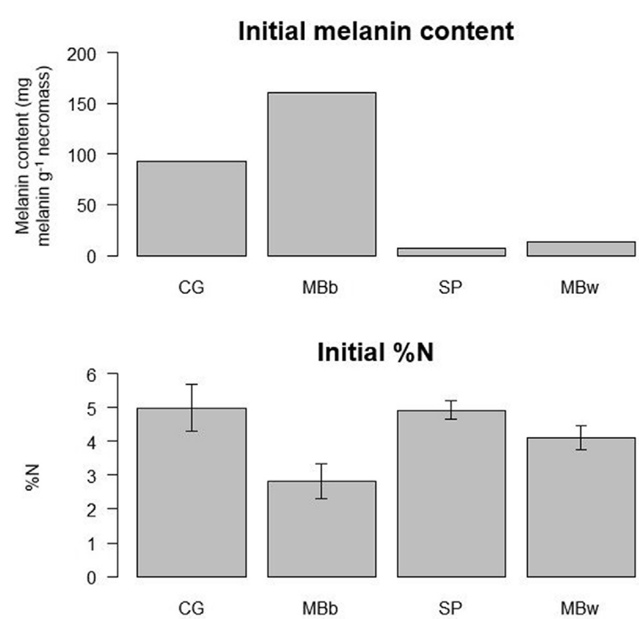

Fig. 1. (a) Initial melanin content (mg melanin g^{-1} necromass) and (b) initial nitrogen content (%N) of four types of necromass. Error bars for melanin content show precision of balance and are too small to see. Error bars for %N show standard deviation of four samples analyzed. CG = *Cenococcum geophilum*; MBb = *Meliniomyces bicolor* – black; SP = *Suillus punctipes*; MBw = *Meliniomyces bicolor* – white.

3.2. Extent of degradation

Mass loss from all four necromass types was rapid at the beginning of incubation and slowed as time progressed. Three types lost more than half the initial mass in the first seven days of incubation: CG lost 74%, SP lost 69%, and MBw lost 64%, on average. After approximately one month of degradation, the mass loss of each type stabilized and, after 90 days, none of the samples were completely degraded. CG, SP, and MBw degraded at essentially the same rate while MBb had lost significantly less mass than the rest of the types at each harvest ($p < 0.05$). MBb lost only 28% of its mass after seven days and 68% after 90 days. The degradation of fungal necromass across species was best represented by a Multi-G model (Fig. 2), suggesting that there were two pools of C degrading simultaneously: a fast- (G_1) and slow-degrading (G_2) pool, respectively.

3.3. Chemical changes during degradation

Aliphatic compounds and carbohydrates made up most of the mass of undegraded necromass of every necromass type, which remained true throughout the degradation sequence. In CG necromass, the relative carbohydrate content decreased after two days of incubation, associated with a brief increase in relative aliphatic content (Fig. 3a and b). Subsequently, relative aliphatic content decreased and relative carbohydrate content increased over the remainder of the incubation. Relative sterol content, while steady for the first week, increased thereafter. MBb necromass contained significantly more aliphatic compounds than the other species before incubation and throughout the degradation sequence ($p < 0.05$). The relative abundances of the different classifications of compounds in the MBb necromass remained fairly constant until the day 28 harvest, at which point relative aliphatic content decreased and relative carbohydrate content increased (Fig. 3c and d). For SP, the relative abundances of the different components remained constant for the first week of degradation (Fig. 3e and f), followed by a decrease in relative aliphatic content and an increase in relative carbohydrate content. The relative sterol content of SP necromass increased after 60 and 90 days, peaking at day 60. During the first four days of incubation of MBw necromass, the relative carbohydrate content decreased (Fig. 3g and h) while there was an increase in the relative abundance of aliphatic compounds. After four days, the relative aliphatic content in Mbw necromass sharply decreased and relative carbohydrate content increased.

The relative abundance of aromatic compounds was also higher at the end of the degradation study than at the beginning for each of the four necromass types (Fig. 4a). Further, for three of the four necromass types, nitrogen content (%N) was lower after 90 days of degradation than the undegraded necromass (Fig. 4b). The FTIR spectra from CG and SP further demonstrated that degraded necromass was distinct from undegraded necromass (Fig. 5). Five peaks were identified in the carbohydrate region of CG and SP necromass, from 1180 to 830 cm^{-1}. In this region, peaks broadened from day 0 to day 90. From the day 0 spectrum it was evident that the carbohydrate region contains five peaks (Fig. 5a,c), whereas, at day 90, this region appears as one large peak and a small peak on either end for both CG and SP necromass (Fig. 5b,d).

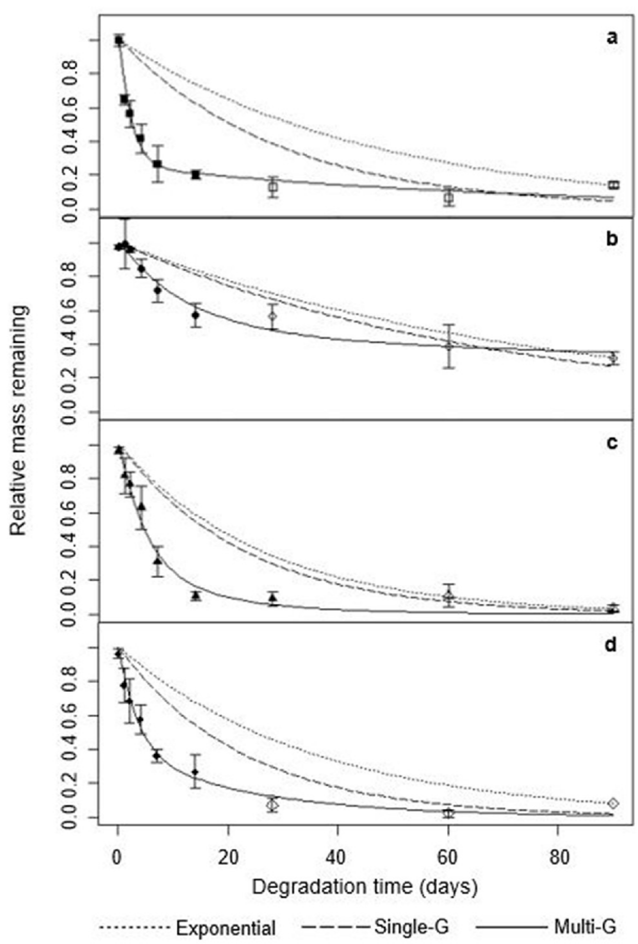

Fig. 2. Necromass mass remaining over 90 days for (a) *Cenococcum geophilum*; (b) *Meliniomyces bicolor* – black; (c) *Suillus punctipes*; and (d) *Meliniomyces bicolor* – white. Error bars show standard deviation. Lines show exponential (dotted), Single-G (dashed), and Multi-G (solid) kinetic models.

4. Discussion

4.1. Extent of degradation

Similar to other studies of fungal necromass degradation, we found that the necromass from all four ECM fungal types degraded rapidly. Our results clearly demonstrate that there can be significant amounts of mass loss even within the first few days of incubation. The very rapid initial mass loss is most likely attributable to abiotic leaching (Maillard et al., in review), which has also been documented during the initial stages of plant-derived organic matter degradation (Webster and Benfield, 1986). The relatively rapid decay we observed may also have been positively influenced by our use of root-excluding litter-bags, which were necessary to facilitate necromass recovery for chemical profiling. Recent research has shown that interactions of fungal tissue with condensed tannins produced by roots (Clemmensen et al., 2013; Adamczyk and Sietio, 2019; Hattenschwiler et al., 2019), which themselves may degrade more slowly than other types of organic matter (Sun et al., 2018), significantly slows the rate of fungal necromass degradation. Although the initial rates of mass loss were high, none of the four necromass types degraded completely by the end of the 90-day degradation period. In our case, we observed minimal mass loss from 28 days onward, suggesting that most mass loss from fungal necromass happens within a month of burial and that remaining mass has the potential to be stored belowground over much longer time scales. These latter results are consistent with the recent study of Fernandez et al. (2019), who found no significant additional mass loss in the following 21 months after the initial 3 month harvest of necromass of four mycorrhizal species, including the same strains of CG and MBb used here. The slight apparent increase in mass remaining of SP from day 28 to day 60

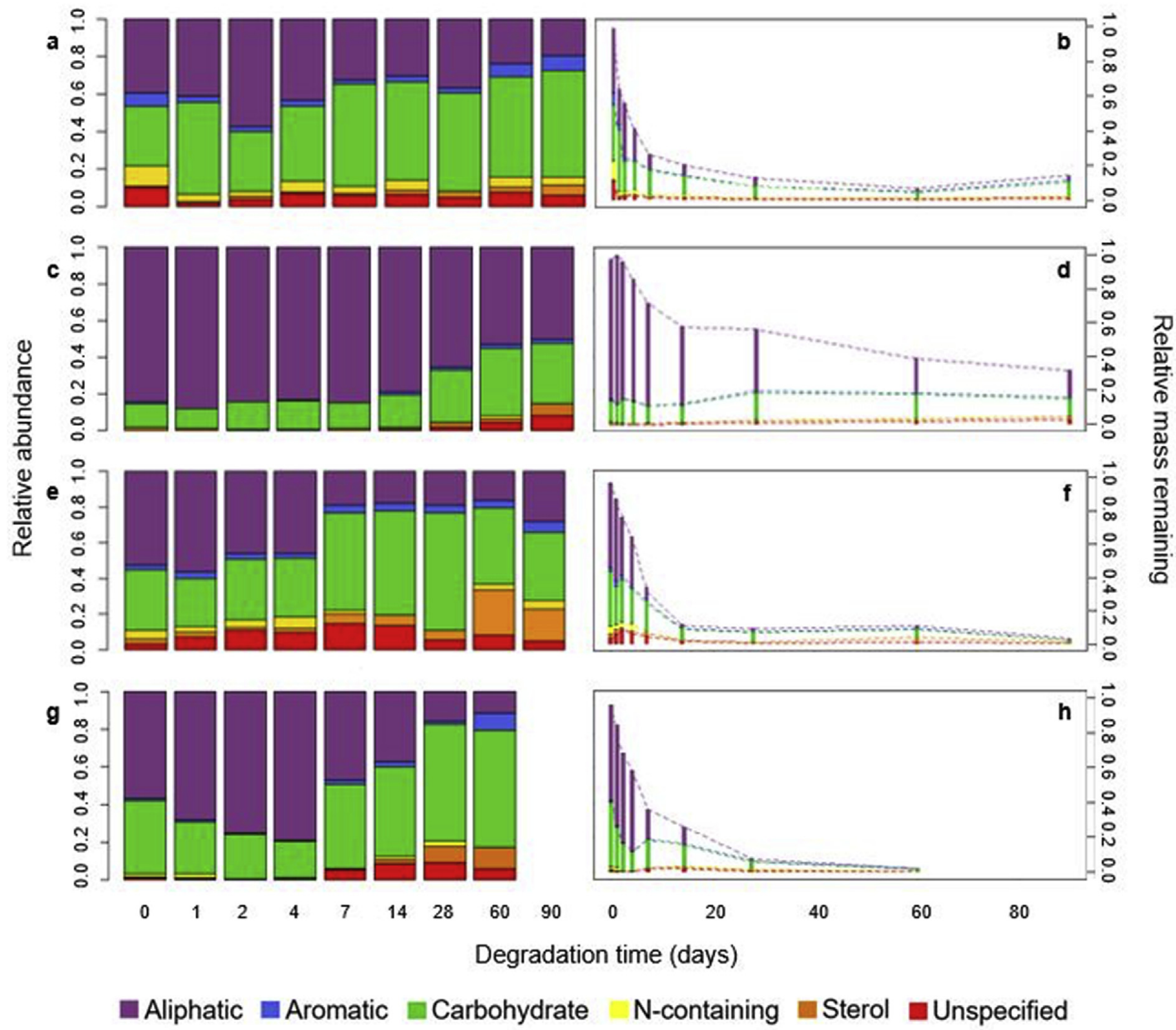

Fig. 3. Bulk chemical changes and chemical changes relative to mass loss for necromass from (a,b) *Cenococcum geophilum*; (c,d) *Meliniomyces bicolor* – black; (e,f) *Suillus punctipes*; (g,h) *Meliniomyces bicolor* – white. *Meliniomyces bicolor* – white was not analyzed by pyGCMS on day 90 due to insufficient mass. Soil is homogenized soil taken from field site. Lines on chemical changes relative to mass loss plots are to guide the eye.

and of CG from day 60 to day 90 in our study is likely an artifact of averaging the harvested and initial masses to account for bag disturbance, though may also be due to the growth of other microbes on the degrading necromass.

With regard to initial melanin and N content, our results support the importance of these two biochemical traits in controlling rates of necromass decomposition, both within and across species. As in previous studies (Fernandez et al., 2019), we found that the concentration of melanin within fungal necromass is a major contributor to the rate of degradation of the slow-degrading necromass pool. Specifically, we found that melanin was significantly negatively correlated to rate constant k_2 ($R^2 = 0.92$, $p < 0.05$; Fig. 6a), but not k_1 ($R^2 = 0.07$, $p > 0.70$; Fig. 6b). We also found that %N and rate constant k_1 were positively correlated ($R^2 = 0.55$, $p > 0.25$; Fig. 6c) and, if SP is omitted, the correlation was highly significant ($R^2 = 0.995$, $p < 0.05$). Conversely, there was a much weaker correlation between %N and k_2 ($R^2 = 0.34$, $p > 0.40$; Fig. 6d). Interestingly, we found that although CG was melanized and appeared dark morphologically, its decomposition was much more rapid than in previous studies (Fernandez and Koide, 2013; Fernandez et al., 2019). If melanin content were the only factor contributing to the rate of degradation, the mass loss of CG necromass should have fallen between MBb and the two lower melanin species. Instead, CG degraded at effectively the same rate as the lower melanin species. These results indicate that without sufficient melanization, the necromass of CG degrades rapidly, likely due to its relatively high N content. Taken together, our findings support other studies showing that broad differences in degradation rates across species can be attributed to initial nitrogen content (Koide and Malcolm, 2009; Brabcová et al., 2018, Certano et al., 2018), while melanin content can be an important contributing factor in differences in degradation rate within a species (Fernandez and Kennedy, 2018).

4.2. Chemical changes in necromass during degradation

There were a wide range of differences in the chemical composition of degraded and undegraded ECM fungal necromass. The consistent decrease in aliphatic content that we observed across the four necromass ECM types has also been documented in the degradation of saprotrophic fungi (Schreiner et al., 2014; Bruner et al., 2016; Certano et al., 2018), plant matter (Wickings et al., 2012), and dairy manure (Calderón et al., 2006). A possible

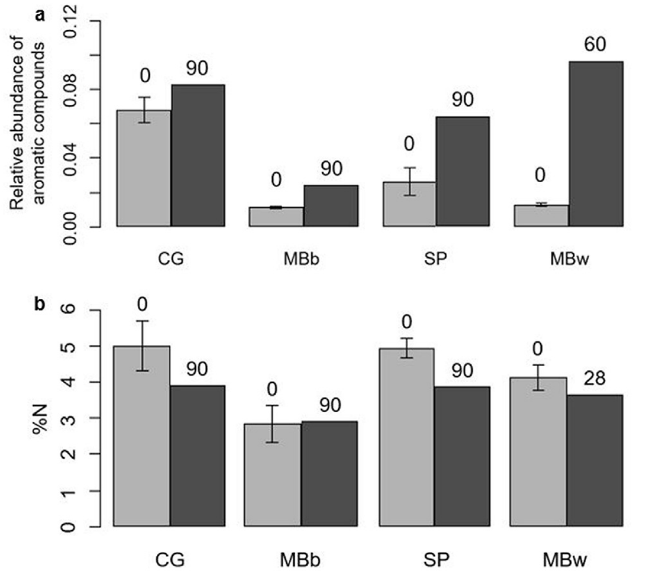

Fig. 4. (a) Relative aromatic content (based on pyGCMS) and (b) nitrogen content (%N, from elemental analysis) of degraded and undegraded necromass. Error bars show standard deviation. No error bars are presented for degraded necromass (days 28. 60, and 90) because there was insufficient mass of degraded necromass to analyze multiple samples with each analytical technique. Number above bar indicates days of degradation. CG = *Cenococcum geophilum*; MBb = *Meliniomyces bicolor* − black; SP = *Suillus punctipes*; MBw = *Meliniomyces bicolor* − white.

explanation for the consistent decrease in aliphatic content across all these organic matter types is the use of fatty acids as a source of energy by microbial decomposers (Calderón et al., 2006).

There are conflicting reports about the decomposition rates of fungal cell wall polysaccharides, especially chitin (Swift et al., 1979; Drigo et al., 2012; Fernandez and Koide, 2012). We observed that ~50% of the cell wall polysaccharides degraded during the first week of degradation for 3 of the 4 types (only 21% for MBb), indicating that a portion of cell wall polysaccharides are lost quickly upon burial (Drigo et al., 2012; Fernandez and Koide, 2012). At the end of the degradation period, however, 5−25% of carbohydrates remained (for CG, SP, and MBw), suggesting that there is a different portion of the carbohydrate pool that is resistant to degradation, as has been shown previously (Swift et al., 1979). We speculate that the latter portion may be complexed with more recalcitrant biopolymers such as melanin (see below).

The relative abundances of aromatic compounds and sterols were higher in necromass that degraded for 90 days (60 days for MBw) than undegraded necromass across types. A relative increase in sterol content was also documented in four species of saprotrophic fungi over a 28-day degradation period (Bruner et al., 2016), and an increase in aromatic content was documented in the degradation of a different saprotrophic species varying in mycelial architecture (Certano et al., 2018). The increase in aromatic content demonstrates that aromatic compounds are more resistant to degradation than the other components, which has been demonstrated for both melanin (Butler and Day, 1998) and lignin (Swift et al., 1979). We believe the increase in sterol content is due not to the recalcitrance of sterols but rather to growth of microbes on the necromass, which has been shown to be rapid (Brabcová et al., 2018). Ergosterol, for example, is a fungal-specific sterol that has been shown to be labile in soil and is therefore a biomarker for living fungus, not degraded necromass (Wallander and Nyland, 1992).

Comparing the different morphotypes of *M. bicolor* suggests that melanin content additionally affects the magnitude of chemical changes as necromass degrades. After just seven days, the degradation of MBw necromass was comparable to MBb necromass after 90 days of degradation, both in terms of chemical composition and mass loss. The chemical changes that occurred as MBw necromass degraded were dynamic, with necromass from each harvest being chemically distinct from the previous harvest, even in the first week of degradation when harvest was frequent. On the contrary, the degradation of MBb necromass was less dynamic; few changes in the relative abundances of the classes of compounds occurred in the first week of MBb necromass degradation. For example, unlike in MBw necromass, there is no decrease in the relative abundance of carbohydrates in MBb necromass over the first four days of degradation. Minimal changes in the chemical composition of MBb necromass, especially in carbohydrate content, suggest that the melanin in MBb could be protecting the other cell wall components, especially carbohydrates, from degradation either physically, chemically, or biologically (Kuo and Alexander, 1967; Bull, 1970; Six et al., 2002; Fernandez et al., 2016). Because MBw necromass contained less melanin than MBb necromass, we speculate the cell wall components of MBw necromass were not protected to the

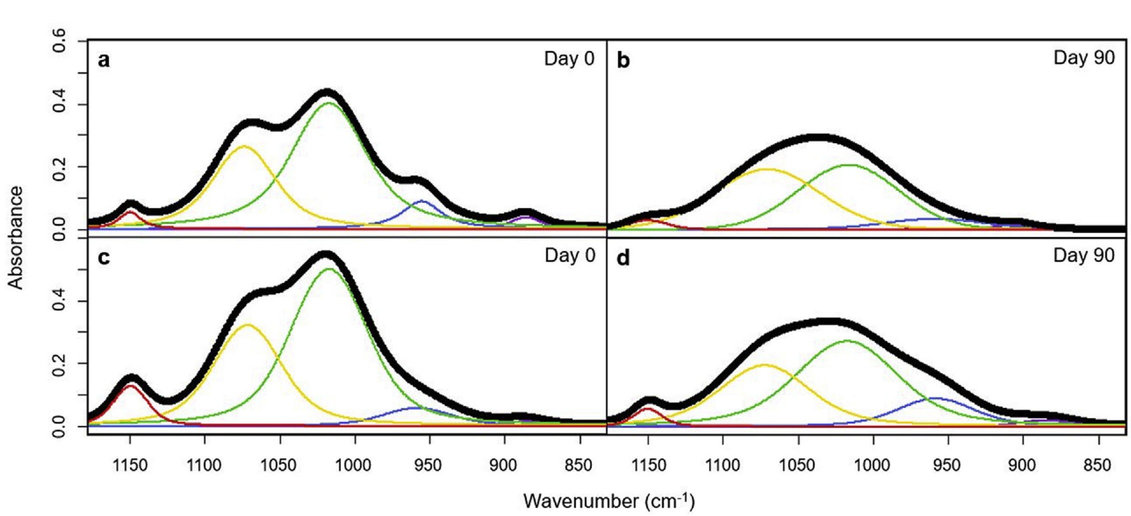

Fig. 5. Carbohydrate region of ATR-FTIR spectra for *Cenococcum geophilum* (a) before (day 0) and (b) after (day 90) degradation and *Suillus punctipes* (c) before and (d) after degradation. Individual peaks were deconvoluted using PeakFit software and are shown as colored peaks under the full FTIR spectra, shown as solid black peaks.

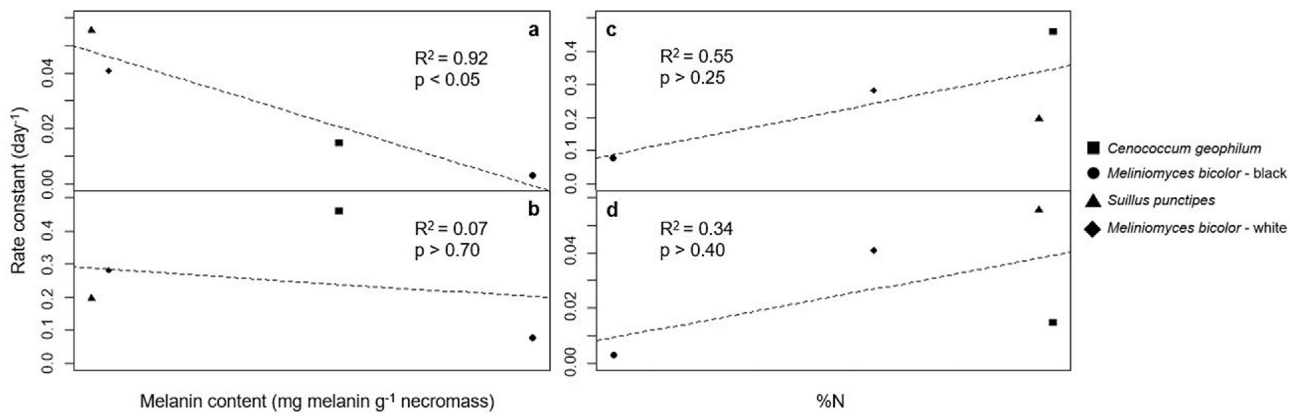

Fig. 6. Melanin content (mg melanin g^{-1} necromass) versus rate constant for (a) slow-degrading pool, k_2 (day^{-1}) ($R^2 = 0.92$; $p < 0.05$) and (b) fast-degrading pool, k_1, ($R^2 = 0.07$, $p > 0.70$), and nitrogen content (%N) versus rate constant for (c) fast-degrading pool, k_1, ($R^2 = 0.55$, $p > 0.25$) and (d) slow-degrading pool, k_2 (day^{-1}) ($R^2 = 0.34$; $p > 0.40$).

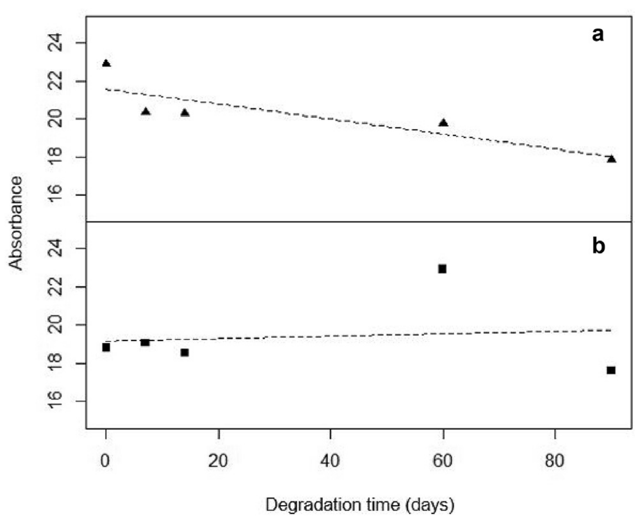

Fig. 7. Peak area of N-glucosamine peak (1072 cm^{-1}) in (a) *Suillus punctipes* necromass ($R^2 = 0.73$, $p < 0.1$) and (b) *Cenococcum geophilum* necromass ($R^2 = 0.01$, $p > 0.8$).

same extent, allowing for more rapid chemical changes.

Our FTIR results indicate that melanin content also appears to directly affect the degradation of chitin. The peak at 1072 cm^{-1} is indicative of N-glucosamine, the monomer of chitin (Pierce and Rast, 1995). In SP necromass, we found that the relative area of this peak decreased with degradation time (Fig. 7a; $R^2 = 0.73$, $p < 0.1$). A similar apparent decrease in this peak was also shown during the degradation of low melanin saprotrophic fungus *Fusarium avenaceum* necromass (Schreiner et al., 2014). In CG necromass, however, we found no correlation between degradation time and this peak area (Fig. 7b; $R^2 = 0.01$, $p > 0.8$). In conjunction, these results suggest that chitin degrades more readily in lower compared to higher melanin-containing necromass. This finding is also consistent with previous work that has demonstrated that melanin slows the degradation of cell wall polysaccharides (Bull, 1970).

4.3. SOM formation

As ECM fungal necromass decomposes, its chemical composition approaches that of stable SOM (Fig. 3), suggesting that ECM fungal necromass is likely an important contributor to this long-term storage pool (Kallenbach et al., 2016). In particular, the soil at our field site was high in aromatics relative to the chemical composition of the fungal necromass (26.8%) and, as highlighted above, the relative abundance of aromatic compounds increased in fungal necromass as degradation proceeded. If we model this increase (starting at day 14) as a linear relationship and as a 2nd order polynomial for each of the four types of fungal necromass, the relative aromatic content of ECM fungal necromass would match that of the soil at our site within 3–7 months for MBw, but may take up to four years for MBb, with CG and SP falling intermediate. Collectively, this suggests that, in as short as three months, fungal necromass could become chemically similar to stable SOM.

5. Conclusions

This study adds to a rapidly growing body of knowledge about the dynamics of ECM fungal necromass decomposition (Fernandez et al., 2016). Unlike previous work, our in-depth characterization of the first week of necromass degradation indicates that chemical changes are notably dynamic, but have some clear consistency across necromass types varying in initial biochemical composition. In particular, there is a consistent decline in aliphatic compounds and a corresponding relative increase in carbohydrates, sterols, and aromatic compounds in degraded necromass. Further, our work reiterates the increasingly well-recognized importance of initial N content and melanin in affecting the rates of necromass decomposition. While our results and others show melanin can strongly slow decomposition and limit chemical changes within a species, it appears that initial N content may be a more general contributor to enhanced decomposition across species. Future field-based work using isotopic labels to trace the specific fates of necromass N and C compounds into various SOM pools will be a key next step in clarifying exactly how fungal necromass degradation contributes to belowground nutrient cycling and C storage.

Acknowledgements

Dr. Elizabeth Austin-Minor provided valuable input on an early version of this manuscript, and two anonymous reviewers also provided comments that significantly improved its quality. Field and laboratory support from Amanda Certano (University of Minnesota Twin Cities) and Julia Agnich (University of Minnesota Duluth) was indispensable. We thank the Cedar Creek Ecosystem Science Reserve for allowing us to use a plot of their land to perform the field degradation study. Funding for this study was provided by the University of Minnesota Duluth to K.M. Schreiner and NSF DEB

Grant 1554375 to P.G. Kennedy.

Supplementary data

Supplementary data to this article can be found online at https://doi.org/10.1016/j.funeco.2020.100922.

References

Adamczyk, B., Sietio, O.-M., 2019. Interaction between tannins and fungal necromass stabilizes fungal residues in boreal forest soils. New Phytol. 223, 16–21. https://doi.org/10.1111/nph.15729 (in press).
Allen, M.F., Kitajima, K., 2013. In situ high-frequency observations of mycorrhizas. New Phytol. 200 (1), 222–228.
Bartnicki-Garcia, S., 1968. Cell wall chemistry, morphogenesis, and taxonomy of fungi. Annu. Rev. Microbiol. 88–108.
Berner, R.A., 1964. An idealized model of dissolved sulfate distribution recent sediments in. Geochem. Cosmochim. Acta 28, 1497–1503.
Brabcová, V., Nováková, M., Davidová, A., Baldrian, P., 2016. Dead fungal mycelium in forest soil represents a decomposition hotspot and a habitat for a specific microbial community. New Phytol. 210 (4), 1369–1381.
Brabcová, V., Štursová, M., Baldrian, P., 2018. Nutrient content affects the turnover of fungal biomass in forest topsoil and the composition of associated microbial communities. Soil Biol. Biochem. 118, 187–198.
Bruner, V.J., Schreiner, K.M., Blair, N.E., Egerton, L., 2016. Chemical Characterization of the Degradation of Necromass from Four Ascomycete Fungi: Implications for Soil Organic Carbon Turnover and Storage. American Geophysical Union. Fall Meeting 2016, abstract #B41D-0462. 2016AGUFM.B41D0462B.
Bull, A.T., 1970. Inhibition of polysaccharases in relation by Melanin : to mycolysis enzyme inhibition. Arch. Biochem. Biophys. 345–356.
Butler, M.J., Day, A.W., 1998. Fungal melanins: a review. Can. J. Microbiol. 44, 1115–1136.
Calderón, F.J., Mccarty, G.W., Reeves, J.B., 2006. Pyrolisis-MS and FT-IR analysis of fresh and decomposed dairy manure. J. Anal. Appl. Pyrol. 76, 14–23.
Certano, A.K., Fernandez, C.W., Heckman, K.A., Kennedy, P.G., 2018. The afterlife effects of fungal morphology: contrasting decomposition rates between diffuse and rhizomorphic necromass. Soil Biol. Biochem. 126, 76–81.
Clemmensen, K.E., Bahr, A., Ovaskainen, O., Dahlberg, A., Ekblad, A., Wallander, H., Stenlid, J., Finlay, R.D., Wardle, D.A., Lindahl, B., 2013. Roots and associated fungi drive long-term carbon sequestration in boreal forest. Science 339, 1615–1618.
Çoban-Yıldız, Y., Fabbri, D., Tartari, D., Tuğrul, S., Gaines, A., 2000. Application of pyrolysis–GC/MS for the characterisation of suspended particulate OM in the Mediterranean Sea: a comparison with the Black Sea. Org. Geochem. 31, 1627–1639.
Drigo, B., Anderson, I.C., Kannangara, G.S.K., Cairney, J.W.G., Johnson, D., 2012. Rapid incorporation of carbon from ectomycorrhizal mycelial necromass into soil fungal communities. Soil Biol. Biochem. 49, 4–10.
Feofilova, E.P., 2010. The Fungal Cell Wall : Modern Concepts of its Composition, vol. 79, pp. 711–720.
Fernandez, C.W., Heckman, K., Kolka, R., Kennedy, P.G., 2019. Melanin mitigates the accelerated decay of mycorrhizal necromass with peatland warming. Ecol. Lett. 22, 498–505.
Fernandez, C.W., Kennedy, P.G., 2018. Melanization of mycorrhizal fungal necromass structures microbial decomposer communities. J. Ecol. 106, 468–479.
Fernandez, C.W., Koide, R.T., 2014. Initial melanin and nitrogen concentrations control the decomposition of ectomycorrhizal fungal litter. Soil Biol. Biochem. 77, 150–157.
Fernandez, C.W., Koide, R.T., 2013. The function of melanin in the ectomycorrhizal fungus *Cenococcum geophilum* under water stress. Fungal Ecol. 6, 479–486.
Fernandez, C.W., Koide, R.T., 2012. The role of chitin in the decomposition of ectomycorrhizal fungal litter. Ecology 93, 24–28.
Fernandez, C.W., Langley, J.A., Chapman, S., Mccormack, M.L., Koide, R.T., 2016. The decomposition of ectomycorrhizal fungal necromass. Soil Biol. Biochem. 93, 38–49.
Fogel, R., Hunt, G., 1983. Contribution of mycorrhizae and soil fungi to nutrient cycling in a Douglas-fir ecosystem. Can. J. For. Res. 13 (2), 219–232.
Godbold, D.L., Hoosbeek, M.R., Lukac, M., Cotrufo, M.F., Janssens, I.A., Ceulemans, R., Polle, A., Velthorst, E.J., Scarascia-Mugnozza, G., De Angelis, P., Miglietta, F., Peressotti, A., 2006. Mycorrhizal hyphal turnover as a dominant process for carbon input into soil organic matter. Plant Soil 281, 15–24.
Hagenbo, A., Clemmensen, K.E., Finlay, R.D., Kyaschenko, J., Lindahl, B.D., Fransson, P., Ekblad, A., 2017. Changes in turnover rather than production regulate biomass of ectomycorrhizal fungal mycelium across a Pinus sylvestris chronosequence. New Phytol. 214 (1), 424–431.
Hattenschwiler, S., Sun, T., Coq, S., 2019. The chitin connection of polyphenols and its ecosystem consequences. New Phytol. 223, 5–7.
Henson, J.M., Butler, M.J., Day, A.W., 1999. The dark side of the mycelium: melanins of phytopathogenic fungi. Annu. Rev. Phytopathol. 447–471.
Högberg, M.N., Högberg, P., 2002. Extramatrical ectomycorrhizal mycelium contributes one-third of microbial biomass and produces, together with associated roots, half the dissolved organic carbon in a forest soil. New Phytol. 154, 791–795.
Jobbagy, E.G., Jackson, R.B., 2000. The vertical distribution of soil organic carbon and its relation to climate and vegetation the vertical distribution of soil organic carbon and its ecological applications. Ecol. Appl. 10 (2), 423–436.
Kallenbach, C.M., Frey, S.D., Grandy, A.S., 2016. Direct evidence for microbial-derived soil organic matter formation and its ecophysiological controls. Nat. Commun. 7, 1–10.
Koide, R.T., Malcolm, G.M., 2009. N concentration controls decomposition rates of different strains of ectomycorrhizal fungi. Fungal Ecol. 2, 197–202.
Kuo, M., Alexander, M., 1967. Inhibition of the lysis of fungi by melanins. J. Bacteriol. 94, 624–629.
López-Mondéjar, R., Brabcová, V., Štursová, M., Davidová, A., Jansa, J., Cajthaml, T., Baldrian, P., 2018. Decomposer food web in a deciduous forest shows high share of generalist microorganisms and importance of microbial biomass recycling. ISME J. 12 (7), 1768.
Maillard F, Andrews A, Schilling J, Kennedy PG, in review. Functional convergence in the decomposition of fungal necromass in wood and soil, FEMS (Fed. Eur. Microbiol. Soc.) Microbiol. Ecol.
Pierce, J.A., Rast, D.M., 1995. A comparison of native and synthetic mushroom melanins by Fourier-transofm infrared spectroscopy. Phytochemistry 39, 49–55.
Prados-Rosales, R., Toriola, S., Nakouzi, A., Chatterjee, S., Stark, R., Gerfen, G., Tumpowsky, P., Dadachova, E., Casadevall, A., 2015. Structural characterization of melanin pigments from commercial preparations of the edible mushroom Auricularia auricula. J. Agric. Food Chem. 63, 7326–7332.
Schreiner, K., Blair, N., Egerton-Warburton, L., Levinson, W., 2014. Contribution of Fungal Macromolecules to Soil Carbon Sequestration. Soil Carbon. Springer International Publishing, Switzerland, pp. 155–161.
Schweigert, M., Herrmann, S., Miltner, A., Fester, T., Kästner, M., 2015. Fate of ectomycorrhizal fungal biomass in a soil bioreactor system and its contribution to soil organic matter formation. Soil Biol. Biochem. 88, 120–127.
Simpson, A.J., Simpson, M.J., Smith, E., Kelleher, B.P., 2007. Microbially derived inputs to soil organic matter: are current estimates too low? Environ. Sci. Technol. 41, 8070–8076.
Six, J., Conant, R.T., Paul, E.A., Paustian, K., 2002. Stabilization mechanisms of soil organic matter : implications for C-saturation of soils. Plant Soil 241, 155–176.
Smiderle, F.R., Olsen, L.M., Ruthes, A.C., Czelusniak, P.A., Sassaki, G.L., Gorin, P.A.J., Iacomini, M., 2012. Exopolysaccharides, proteins and lipids in Pleurotus pulmonarius submerged culture using different carbon sources. Carbohydr. Polym. 87, 368–376.
Sun, T., Hobbie, S.E., Berg, B., Zhang, H., Wang, Q., Wang, Z., Hattenschwiler, S., 2018. Contrasting dynamics and trait controls in first-order root compared with leaf litter decomposition. Proc. Natl. Acad. Sci. Unit. States Am. 115 (4), 10392–10397.
Swift, M.J., Heal, O.W., Anderson, J.M., 1979. Decomposition in Terrestrial Ecosystems. Blackwell, Oxford.
van der Wal, A., Bloem, J., Mulder, C., de Boer, W., 2009. Relative abundance and activity of melanized hyphae in different soil ecosystems. Soil Biol. Biochem. 41 (2), 417–419.
Wallander, H, Nyland, J.E, 1992. Effects of excess nitrogen and phosphorus starvation on the extramatrical mycelium of Pinus sylvestrus L. ectomycorrhiza. New Phytol. 120, 495–503.
Webster, J.R., Benfield, E.F., 1986. Vascular plant breakdown in freshwater ecosystems. Annu. Rev. Ecol. Systemat. 17, 567–594.
Westrich, J.T., Berner, R.A., 1984. The role of sedimentary organic matter in bacterial sulfate reduction : the G model tested. Limonl. Oceanogr. 29, 236–249.
Wickings, K., Grandy, A.S., Reed, S.C., Cleveland, C.C., 2012. The origin of litter chemical complexity during decomposition. Ecol. Lett. 15, 1180–1188.